Applications of optical coherence tomography in the non-contact assessment of automotive paints

Samuel Lawman[a,b], Jinke Zhang[a], Bryan M. Williams[b], Yalin Zheng[b] and Yao-Chun Shen*[a]
[a] Department of Electrical Engineering and Electronics, University of Liverpool, Liverpool L69 3GJ, UK; [b] Department of Eye and Vision Science, University of Liverpool, Liverpool L7 8TX, UK

ABSTRACT

The multiple layer paint systems on modern cars serve two end purposes, they firstly protect against corrosion and secondly give the desired visual appearance. To ensure consistent corrosion protection and appearance, suitable Quality Assurance (QA) measures on the final product are required. Various (layer thickness and consistency, layer composition, flake statistics, surface profile and layer dryness) parameters are of importance, each with specific techniques that can measure one or some of them but no technique that can measure all or most of them. Optical Coherence Tomography (OCT) is a 3D imaging technique with micrometre resolution. Since 2016, OCT measurements of layer thickness and consistency, layer composition fingerprint and flake statistics have been reported. In this paper we demonstrate two more novel applications of OCT to automotive paints. Firstly, we use OCT to quantify unwanted surface texture, which leads to an "orange peel" visual defect. This was done by measuring the surface profiles of automotive paints, with an un-optimised precision of 37 nm over lateral range of 7 mm, to quantify texture of less than 500 nm. Secondly, we demonstrate that OCT can measure how dry a coating layer is by measuring how fast it is still shrinking quasi-instantaneously, using Fourier phase sensitivity.

Keywords: Optical Coherence Tomography, automotive, car, coatings, profilometry, drying, functional imaging, phase sensitivity

1. INTRODUCTION

Most modern vehicles are protected by multi-layered coating systems, which have been developed and become more complex over 100+ years[1]. The need for the multiple different coatings comes from the requirement to protect the majority steel bodies from corrosion and damage from a variety of physical (e.g. stone chipping and UV induced chemical breakdown) and chemical (e.g. road salt enhanced oxidation of steel and etching by acids in bird droppings) environmental attacks. The lower layers currently commonly consist of electroplated galvanisation, location specific layers with specific tasks and a primer coat. This paper is focused on the topcoats of automotive paint systems. As well as protection, these layers provide most of the aesthetic properties and consist of a coloured base coat, which may or may not contain metallic or mica flakes, and clear top coat, which provides the final layer of protection and the surface gloss.

To ensure consistent appearance and protection from the topcoats applied in an automobile factory or body repair shop, the measurement of several parameters could be of use to the Quality Assurance process. The first of these is the applied dry thickness of each coating. There are three types of handheld single point devices currently widely used[2]. Magnetic and eddy current probes are low cost, and it can give the total thickness of a coating system on metallic substrates, while ultrasound probes are more expensive but work independent of substrate and are able to measure the thickness of each layer simultaneously. The second parameter is the consistency of layer thickness. Currently this will be assessed by multiple single point measurements and inspection for visual differences. Remote ultrasound[3] and Terahertz Pulse Imaging (TPI)[4] are potential techniques to measure thickness over an area, though both would be high cost and complexity. The third parameter is the compositional consistency of the base coat layer, variances here are most likely to be apparent to a visual inspection. Alternatively, spectroscopic type methods[5], including TPI[6], could be able to quantify composition. The fourth parameter is the size, density and orientation statistics of metallic or mica flakes within the base coat layer. This impacts the visual appearance and, again, an effective quality assurance measure would be visual comparison. It has been shown that orientation and size of metallic particles can be measured directly with confocal microscopy[7]. The fifth parameter is the surface profile. Due to the levelling properties of coatings during application, high spatial frequency roughness is not possible without extreme failures in other parameters or damage sustained after

production. However, low spatial frequency surface texture is prevalent on automobile paintwork. This can be caused by the clear coat being unable to level low spatial frequency texture present on the underlying coatings and/or substrate, uneven initial application of the coating, which again low frequency components cannot be levelled, or dynamic processes that occur in the drying of the layer, such as Bernard-Marragoni cells[8]. Due to the cost of eliminating completely, some texture in generally tolerated. However, changes to or issues with the application process can make the texture unacceptably worse. As part of the QA process to keep the texture consistent and acceptable, surface profile statistics provide quantifiable measures. Optical pattern projection techniques[9] (Moire profilometry) are able to measure the surface profile over large areas and automatically detect product faults. The sixth parameter, which is useful for the direct management of the coating process, is the wetness of applied layers. Most applied automotive coating will include a solvent of some kind (including water), which will evaporate during the drying process causing the layer to thin. As the layer becomes drier, the evaporation and thinning rates will decrease. Hence, a quasi-instantaneous measurement of the rate of thinning is a quantitative measure of how dry it is. There are a variety of contact and non-contact methods that can measure coating dryness, including TPI[10]. In summary, there are multiple informative parameters that can be measured as part of the QA procedures for automotive topcoats, each with different methods of measuring. If one instrument could measure all, or the majority, of these parameters with relatively low cost, it would have a higher chance of being adopted commercially.

Optical Coherence Tomography[11] is a technique that has proliferated exponentially since its original development in 1991[12]. Beyond its original applications in medicine it is finding an ever-increasing amount of applications in other fields[13]. In 2016 two papers[14,15] were published specifically looking at the topcoats of automotive paint systems. The 3D imaging, and functional imaging, capabilities of OCT means that it is able to measure all the parameters described above. Table 1 gives the list of parameters and where their measurements have been (will be) demonstrated with OCT. The measurement of clear coat and, in the majority of cases, base coat thickness has been demonstrated. The benefit over the current widely used methods, is that it is non-contact. 2D (B-Scan) or 3D OCT image data means that consistency of the coating over a length or area can be assessed. The properties of OCT image signal decay through a scattering layer is dependent on the particle concentration and properties, so a correct composition should have specific signal decay fingerprint. However, the signal properties will also be dependent instrumentation properties, so in practice quantitative comparison between results may not be straightforward. The accurate measurement of flake properties is dependent on lateral resolution, however, currently there is active research on this with appropriate OCT systems. This leaves surface profilometry and dryness, in this paper preliminary methods and results for measuring these with OCT will be presented.

Table 1. Automobile topcoat parameters that can be measured with OCT instruments.

Parameter	OCT study
1. Coating thickness	Dong et al[14], Zhang et al[15]
2. Thickness consistency	Dong et al[14], Lawman et al[16]
3. Base coat fingerprint	Zhang et al[15]
4. Flake statistics	Dong et al (flake size only, limited lateral resolution)[14], Zhang et al (Manuscript in preparation)[17]
5. Surface Profile	Preliminary method and results presented in this paper
6. State of Drying	Preliminary method and results presented in this paper

Surface profile measurements using time domain interferometers[18,19], Line Field (LF) Fourier domain OCT like[20,21] and scanning point Fourier domain OCT[22,23] devices are well established. For any interferometer device there are two primary methods of extracting accurate interface positions, phase and envelope. For time domain interferometers, the phase method of phase shifting interferometry[17] can be used to get high precision measurements. However, for height differences greater than 1/4 of the wavelength the technique can suffer with phase ambiguity errors due to the method only measuring relative, rather than absolute, heights. To overcome this the envelope method of white light interferometry[18] can be used instead, using a broadband (low temporal coherence) source, the sample is scanned relative to the reference mirror and the central (maximum) position of the interference signal is found. This returns the absolute position, so does not suffer from phase ambiguity errors. However, the precision of envelope methods is generally worse than phase methods. To obtain the best of both techniques, they can be combined[24]. Likewise, for Fourier domain OCT

or OCT like devices, surface position can be measured by phase methods[20] or envelope methods OCT[19,22,23]. The performance of both methods, for car paint samples, will be compared in this paper. Again the ideal method would combine the two pieces of information, which will be partly explored in this paper.

As well as high sensitivity to spatially relative displacements for profilometry, the Fourier phase is highly sensitive to temporally relative displacements. LF-OCT has previously been used to image pressure-induced displacement of porcine corneas[25] and measure thermal expansion in materials[26]. Here we will use this nm sensitivity to quasi-instantaneously measure the time-dependent thinning rate of a drying solvent varnish coating, comparable to automotive clear coats.

2. METHODS

The LF-OCT system used in this preliminary study has been previously described in Lawman et al, 2016[27]. For this work the Neo sCMOS camera, 75mm Achromatic (AC) objective and 100 mm AC collection lenses, and 300 l/mm grating (800 nm central wavelength) were used in the system to give a maximum lateral range of approximately 10mm and an axial resolution of approximately 2.8 μm. The lack of moving parts of LF-OCT ensures positional stability between measurements and reduces sources of internal vibrations, compared with conventional scanning point systems. Both of these factors will decrease the noise of the surface profile and drying rate measurements described. Methods of reducing the cost of an LF-OCT instrument, to be competitive as a QA instrument in the automotive industry, has been discussed in Lawman et al, 2017[16].

For non-zero padded Fourier domain OCT systems, such as the one used here, the axial Point Spread Function (PSF) (coherence envelope) consists of around 5 data points (pixels) of significant signal. To measure surface axial position by finding the centre of the coherence envelope, "edge detection"[23] was used. OCT axial PSFs generally approximate Gaussian functions, which when converted to log (dB) units become square functions. The gradient of this then is a linear function, which passes through 0 at the centre. Hence, the position of the centre can then be calculated with high precision, using the largest value pixel and the pixel either side, by

$$x_c = x_{1.5} + \frac{\Delta S_{2-1}}{\Delta S_{3-2} - \Delta S_{2-1}} . (\Delta x)$$

where $x_{1.5}$ is the position equidistant of the first and second (largest value) pixel, ΔS_{a-b} is the value of pixel a minus pixel b and Δx is the pixel spacing. For smooth interfaces with high signal to noise, experimental results given in table 2.2.4.2 of Lawman[28] for a scanning point Fourier domain OCT, the method has marginally better precision performance than a 5 point least square Gaussian function fit[22,29] but, more importantly, it is much quicker computationally.

In Fourier domain OCT, the product of the discrete Fourier transform is complex with the magnitude of each pixel taken for structural imaging. The complex phase angle, of each pixel, is known as the Fourier phase and is sensitive to displacement in the same manner as time domain interferogram phase. Figure 1 describes the algorithm used to calculate the Fourier phase profile. The resultant phase values can be converted to relative position by multiplication by $\lambda_c/4\pi$, where λ_c is the central wavelength. For the initial work on combining the benefits of the envelope and phase methods for the car paint surfaces, the envelope position was converted to equivalent phase by multiplication by $4\pi/\lambda_c$. The appropriate multiples of 2π were then added to the phase profile values to minimise the difference between. This is the equivalent of stages up to Fig. 4 (c) in Harasaki et al[24]. Issues with the final stage of the process, the correction of remaining 2π phase ambiguities, are discussed in the results section.

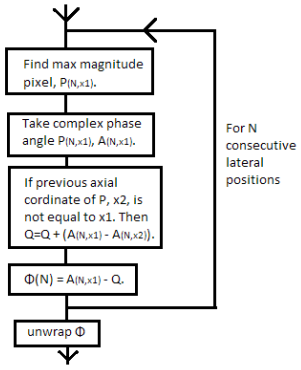

Figure 1. Calculation of surface Fourier phase profile.

To assess the performance of the profilometry methods, firstly a flat surface (flat side of a plano-convex lens) was used to quantify the precision of the envelope and phase methods. To demonstrate the applicability to measure the surface texture ("orange peel") of the clear coat of automotive paints, two sample metallic automotive paint system panels (Santorini Black and Indus Silver), with observable surface texture, and the surface of a plastic lens case, with less observable texture, were measured.

To demonstrate the potential of LF-OCT to measure the drying rate, hence dryness, of coatings, a clear solvent varnish (generic commercial nail varnish) was brushed onto a glass microscope slide and measured every minute. A sample of results up to 20 min is presented here. Each measurement consisted of 10 images taken in approximately one second, short enough to be considered quasi-instantaneous. The peak pixels of the two interfaces of the varnish coating were found by a graph search[30] algorithm, using an inverted amplitude energy function. For each lateral position, firstly the difference of the Fourier phase of the two pixels was taken. Secondly, the value for the first frame was then subtracted from the values for all the frames. Thirdly, the phase change over the 10 frames was then unwrapped. Finally the gradient of phase change over the 10 frames was found by fitting a linear function. These gradients were then converted to optical thickness change rate by multiplication by $\lambda_c/(\Delta t.4\pi)$, where Δt is the time between frames.

3. RESULTS

Figure 2 Top shows the measured flat surface profile calculated by the envelope and phase methods, respectively, from the same single frame measurement. Figure 2 Bottom is the plot of the correlation between the profile heights of the two methods, which is found to be negligible, R=0.37. This indicates the apparent texture (i.e. error as the surface is assumed perfectly flat) is not due to physical distortion between the sample and reference surfaces or vibrations, but due to the methods. Optical imperfections, including sample surface not being at the focal plane (If the Linnik interferometer, of this instrument, is setup perfectly the focal plane will be at the zero path length. A measured sample will always be displaced to this.), optical aberrations (particularly significant in the Czerny-Turner spectrograph) and dust/dirt on optical components throughout the system, could influence either or both methods. The instrument has been developed for imaging; no additional work has been done to optimise it further for profilometry. For the envelope method, this single measurement smooth surface rms error (37 nm) is better than reported equivalent values, which we are currently aware of, for single (157 nm[28]) or averaged (55 nm[29]) B-Scan images with scanning point Fourier domain OCT. The reason for the improvement over scanning point systems, is likely to be the increased stability given by LF-OCT having no moving parts. However, the error is still an order of magnitude higher than typical specialised full field time domain white light interferometry profilometers. Hence, it is likely with refinement the errors reported here could be improved upon. However, as is demonstrated below, this 37 nm precision over the profile length of 7 mm is sufficient to quantify the surface texture of car paints. The error of the phase method is better (23 nm). We are not currently aware of equivalent values reported for scanning point Fourier domain OCT systems. For LF-OCT like setup, but calculating phase of a single interface signal before Fourier transformation, an error of less than 6 nm has been reported[21] and full field time domain phase shifting interferometers are typically an order of magnitude better. So again, improvements on the values found by this preliminary study could be expected with further refinement. However, the failure of the phase method in this study was due the inability to resolve phase ambiguities, which is described below.

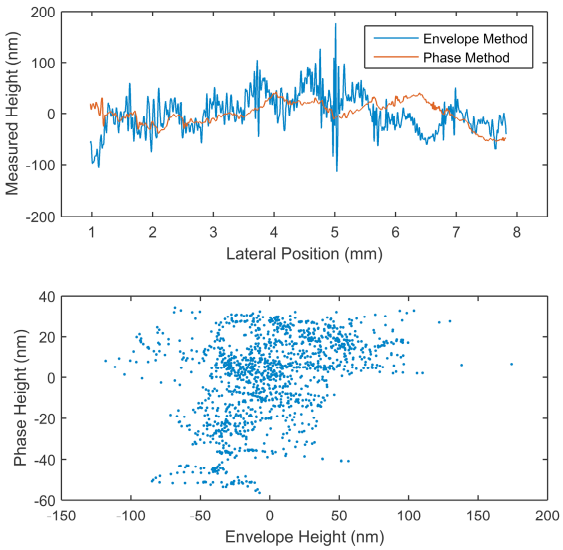

Figure 2. Top – Measured surface profile of flat surface, from same un-averaged B-Scan image data, by the envelope and phase methods, rms values 37 and 23 nm respectively. Bottom – Plot of the negligible correlation between the phase and envelope values, R = 0.37.

Figure 3 Top is an example profile measurement of the Santorini Black sample, from one B-Scan image, with the two methods. The envelope method is robust and returns an accurate surface profile. However, the initial unwrapped phase profile suffers from phase ambiguities and the returned profile is significantly distorted and misleading. Applying the first step of correction, using the envelope values, still results in a profile significantly worse than the envelope function on its own. Figure 3 Middle shows the phase values of this partly corrected profile, with Figure 3 Bottom showing the differential value. There are two illustrative areas, highlighted A and B, that show separate issues. In area A, the jumps in the profile are clear 2π ambiguity errors, which should be reasonably straightforward to correct for with an automated algorithm. However, in area B the signal is the jumps in the profiles are not clear and much more like random noise. In this location the envelope method (Top black) also suffers from increased noise, implying an underlying decrease in the effective signal to noise of the data in this location. Further work is needed to find the cause and solve this issue. For the rest of this paper, the "edge detection" envelope method has been used due to its higher inherent robustness compared to the phase method.

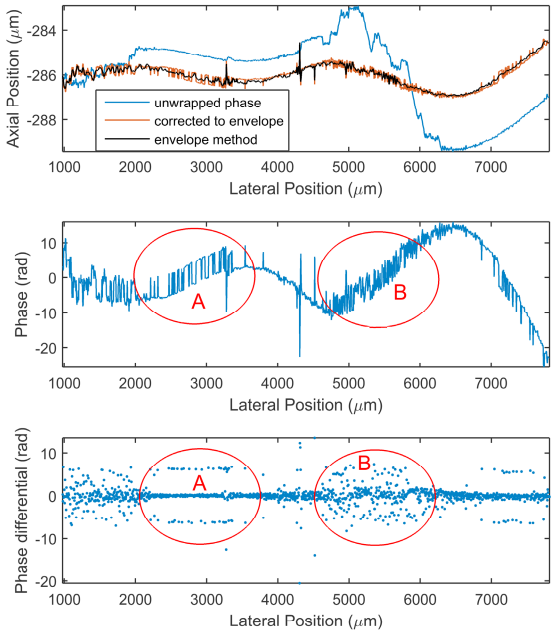

Figure 3. Top - Example profiles obtained from a single B-Scan image obtained by envelope, phase and phase with the first stage of combined ambiguity correction methods. Phase values (Middle), and its differential (Bottom), of partly corrected profile. Two areas, A and B, with different issues are highlighted.

Figure 4 Top shows the surface profile measurements taken at 10 locations and orientations on the Santorini Black sample. The low spatial frequency surface texture on the sample is apparent in these profiles. The smaller higher spatial frequency components of the measured profiles consist of the measurement error and, dust and scratches. Figure 4 Bottom gives is a comparison of example profiles for the three samples measured, with table 2 giving the mean and standard deviation of the measured rms values. The mean rms values indicate that the Santorini Black sample has the most surface texture and the lens case the least.

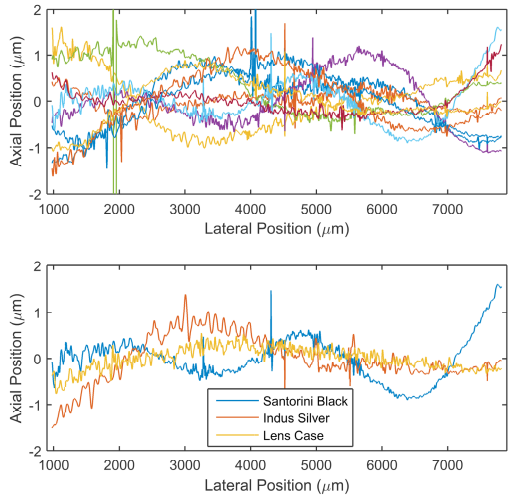

Figure 4. Top - measured surface profiles of the Santorini Black sample, at 10 different locations and orientations. Bottom – example profiles for the three samples measured.

Table 2. Measured rms texture values for the three samples.

Sample	Mean of measured rms texture (nm)	Standard Deviation of measured rms texture	Measurements (N)
Santorini Black	500	160	9
Indus Silver	410	100	5
Lens Case	330	140	5

Figure 5 Top shows the OCT image of the initial measurement of the nail varnish applied to a glass microscope slide. There is significant texture from the brush application, which partially levels out rapidly. Red lines show the peak signal positions, found by a graph search algorithm, of each interface. These are used for the phase measurement of drying rate. Figure 5 Bottom shows the measured drying rates, across the B-Scan images, at five different times. In the initial measurement, the effect of the levelling is seen in the drying rate profile, with differences in magnitude corresponding to peaks lowering and troughs filling. At 1 minute, the levelling effect has reduced and the thinning rate is reasonably consistent (~150 n.nm/s) across the B-Scan. At 2 minutes, there is a small uniform reduction in the drying rate, but by five minutes the thinning has reduced substantially. At 20 minutes the thinning rate is negligible compared to the initial rate. Further work is required to investigate the application of this technique to the later stages of simple solvent coating and practical feasibility for real automotive coatings. Though the errors in these results appear small, they have not yet been quantified.

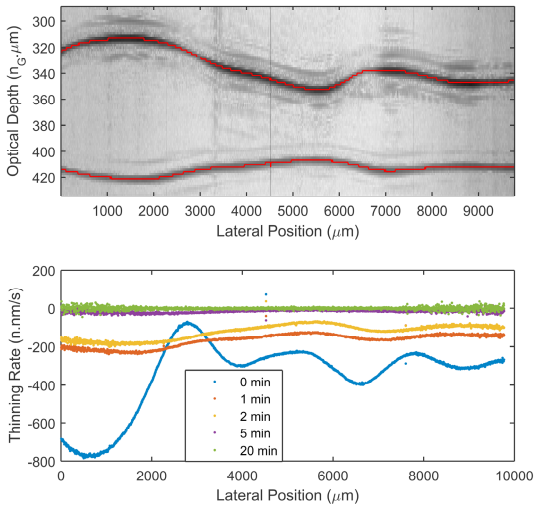

Figure 5. Top – Initial OCT image of nail varnish brushed on a glass microscope slide. The red lines mark the peak pixels for each interface, found with a graph search algorithm. Bottom – quasi-instantaneous thinning rates at four times, measured utilising the Fourier phase of the peak pixels over consecutively taken images.

4. CONCLUSION

Automotive coatings are a new application area for OCT with high potential. Compared with other current and potential techniques for QA and research, the high resolution cross sectional, or 3D, imaging and functional data could be used to measure multiple parameters of interest. Coating thickness and consistency, layer scattering fingerprints and flake statistics are active area of research. To this, here we add surface texture quantification and quasi-instantaneous drying rates. Using a LF-OCT system, our preliminary results demonstrate the feasibility and potential of these measurements. There is still further work required to develop, explore and detail the capabilities of these methods fully. Future OCT devices, built specifically for the automotive industry, that simultaneously quantify several parameters are a possibility.

ACKNOWLEDGEMENTS

The Ultrasensitive Optical Coherence Tomography Imaging for Eye Disease is funded by the National Institute for Health Research's i4i Programme. This paper summarises independent research funded by the National Institute for Health Research (NIHR) under its i4i Programme (Grant Reference Number II-LA-0813-20005). The views expressed are those of the authors and not necessarily those of the NHS, the NIHR, or the Department of Health. This work is partly supported by the UK EPSRC Research Grant No. EP/L019787/1. The authors thank Roy Donga of Jaguar Land Rover Limited for providing the test samples.

REFERENCES

[1] Akafuah, N. K. *et al.* Evolution of the Automotive Body Coating Process-A Review. *Coatings* **6**, doi:10.3390/coatings6020024 (2016).
[2] Brasunas, J. C., Cusham, G. M. & Lakew, B. in *The Measurement, Instrumentation and Sensors: Handbook* (ed John G. Webster) (CRC Press, 1999).
[3] White, J. S., LaPlant, F. P., Dixon, J. W., Emch, D. J. & Datillo, V. P. Non-Contact Real-Time Film Thickness Gage for Automotive Body Painting Applications. Report No. 0148-7191, (SAE Technical Paper, 1998).
[4] Su, K., Shen, Y. C. & Zeitler, J. A. Terahertz Sensor for Non-Contact Thickness and Quality Measurement of Automobile Paints of Varying Complexity. *Ieee Transactions on Terahertz Science and Technology* **4**, 432-439, doi:10.1109/tthz.2014.2325393 (2014).
[5] Muehlethaler, C., Massonnet, G. & Esseiva, P. The application of chemometrics on Infrared and Raman spectra as a tool for the forensic analysis of paints. *Forensic Science International* **209**, 173-182 (2011).
[6] Shen, Y., Taday, P. & Pepper, M. Elimination of scattering effects in spectral measurement of granulated materials using terahertz pulsed spectroscopy. *Applied Physics Letters* **92**, 051103 (2008).
[7] Kirchner, E. & Houweling, J. Measuring flake orientation for metallic coatings. *Progress in organic coatings* **64**, 287-293 (2009).
[8] Abbasian, A., Ghaffarian, S., Mohammadi, N., Khosroshahi, M. & Fathollahi, M. Study on different planforms of paint's solvents and the effect of surfactants (on them). *Progress in organic coatings* **49**, 229-235 (2004).
[9] Loferer, H. P8. 7-Automatic Painted Surface Inspection and Defect Detection. *Proceedings SENSOR 2011*, 871-873 (2011).
[10] Yasui, T., Yasuda, T., Sawanaka, K.-i. & Araki, T. Terahertz paintmeter for noncontact monitoring of thickness and drying progress in paint film. *Applied Optics* **44**, 6849-6856 (2005).
[11] Brezinski, M. E. *Optical Coherence Tomography: Principles and Applications*. (Elsevier Science, 2006).
[12] Huang, D. *et al.* Optical Coherence Tomography. *Science* **254**, 1178-1181, doi:10.1126/science.1957169 (1991).
[13] Stifter, D. Beyond biomedicine: a review of alternative applications and developments for optical coherence tomography. *Applied Physics B-Lasers and Optics* **88**, 337-357, doi:10.1007/s00340-007-2743-2 (2007).
[14] Dong, Y. *et al.* Nondestructive analysis of automotive paints with spectral domain optical coherence tomography. *Applied Optics* **55**, 3695-3700, doi:10.1364/ao.55.003695 (2016).
[15] Zhang, N. *et al.* Characterization of automotive paint by optical coherence tomography. *Forensic Science International* **266**, 239-244, doi:10.1016/j.forsciint.2016.06.007 (2016).
[16] Lawman, S., Williams, B. M., Zhang, J., Shen, Y.-C. & Zheng, Y. Scan-Less Line Field Optical Coherence Tomography, with Automatic Image Segmentation, as a Measurement Tool for Automotive Coatings. *Applied Sciences* **7**, 351 (2017).
[17] Zhang, J. *et al. Non-destructive Analysis of Flakes in Automotive Paints with Time-domain Full-field Optical Coherence Tomography* (2017).
[18] Schreiber, H. & Bruning, J. H. in *Optical Shop Testing* (ed D. Malacara) (John Wiley and Sons Inc, 2007).
[19] Lee, B. S. & Strand, T. C. Profilometry with a coherence scanning microscope. *Applied optics* **29**, 3784-3788 (1990).
[20] Endo, T., Yasuno, Y., Makita, S., Itoh, M. & Yatagai, T. Profilometry with line-field Fourier-domain interferometry. *Optics Express* **13**, 695-701, doi:10.1364/opex.13.000695 (2005).
[21] Reolon, D., Jacquot, M., Verrier, I., Brun, G. & Veillas, C. Broadband supercontinuum interferometer for high-resolution profilometry. *Optics Express* **14**, 128-137, doi:10.1364/opex.14.000128 (2006).

[22] Lawman, S. & Liang, H. D. in *O3A - Optics for Arts, Architecture, and Archaeology Conference II.* (2009).
[23] Amaral, M. M. *et al.* in *SPIE Europe Optical Metrology.* 73900Z-73900Z-73908 (International Society for Optics and Photonics).
[24] Harasaki, A., Schmit, J. & Wyant, J. C. Improved vertical-scanning interferometry. *Applied optics* **39**, 2107-2115 (2000).
[25] De la Torre-Ibarra, M. H., Ruiz, P. D. & Huntley, J. M. Double-shot depth-resolved displacement field measurement using phase-contrast spectral optical coherence tomography. *Optics Express* **14**, 9643-9656, doi:10.1364/oe.14.009643 (2006).
[26] Zhang, Y. *et al.* Measurement of depth-resolved thermal deformation distribution using phase-contrast spectral optical coherence tomography. *Optics express* **23**, 28067-28075 (2015).
[27] Lawman, S. *et al.* High resolution corneal and single pulse imaging with line field spectral domain optical coherence tomography. *Optics Express* **24**, 2395-2405, doi:10.1364/oe.24.012395 (2016).
[28] Lawman, S. J. *Optical and material properties of varnishes for paintings*, Nottingham Trent University, (2011).
[29] Lawman, S. & Liang, H. D. High precision dynamic multi-interface profilometry with optical coherence tomography. *Applied Optics* **50**, 6039-6048, doi:10.1364/ao.50.006039 (2011).
[30] Boykov, Y., Veksler, O. & Zabih, R. Fast approximate energy minimization via graph cuts. *IEEE Transactions on pattern analysis and machine intelligence* **23**, 1222-1239 (2001).